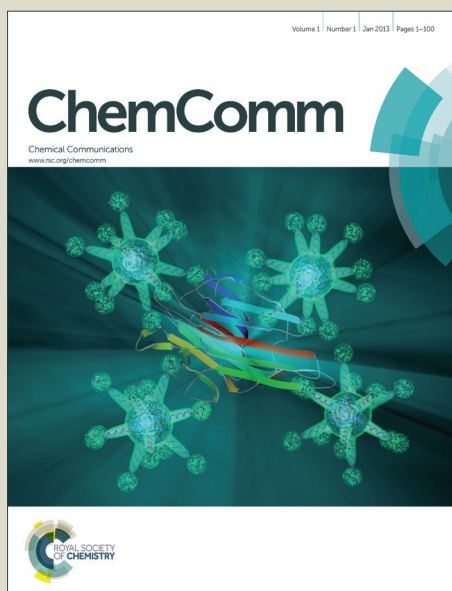


# ChemComm

Accepted Manuscript



This article can be cited before page numbers have been issued, to do this please use: X. Zhou, R. Lai, J. R. Beck, H. Li and C. I. Stains, *Chem. Commun.*, 2016, DOI: 10.1039/C6CC05717A.



This is an *Accepted Manuscript*, which has been through the Royal Society of Chemistry peer review process and has been accepted for publication.

*Accepted Manuscripts* are published online shortly after acceptance, before technical editing, formatting and proof reading. Using this free service, authors can make their results available to the community, in citable form, before we publish the edited article. We will replace this *Accepted Manuscript* with the edited and formatted *Advance Article* as soon as it is available.

You can find more information about *Accepted Manuscripts* in the [Information for Authors](#).

Please note that technical editing may introduce minor changes to the text and/or graphics, which may alter content. The journal's standard [Terms & Conditions](#) and the [Ethical guidelines](#) still apply. In no event shall the Royal Society of Chemistry be held responsible for any errors or omissions in this *Accepted Manuscript* or any consequences arising from the use of any information it contains.



Journal Name

COMMUNICATION

## Nebraska Red: A Phosphinate-Based Near-Infrared Fluorophore Scaffold for Chemical Biology Applications †

Received 00th January 20xx,  
Accepted 00th January 20xxXinqi Zhou,<sup>a</sup> Rui Lai,<sup>a,b</sup> Jon R. Beck,<sup>a</sup> Hui Li,<sup>a,b</sup> and Cliff I. Stains<sup>a,\*</sup>

DOI: 10.1039/x0xx00000x

www.rsc.org/

**A series of novel phosphinate-based dyes displaying near-infrared fluorescence (NIR) are reported. These dyes exhibit remarkable photostability and brightness. The phosphinate functionality is leveraged as an additional reactive handle in order to tune cell permeability as well as provide a proof-of-principle for a self-reporting small molecule delivery vehicle.**

Fluorophores can be used as optical “paints” to visualize otherwise invisible structures or processes. Due to this property, fluorophores have been intensely studied for over 70 years.<sup>1-2</sup> More recently, fluorophores that absorb and emit light within the NIR window (650 nm - 900 nm)<sup>3</sup> have attracted attention for bioimaging applications since NIR wavelengths have deeper tissue penetration and mitigate issues associated with autofluorescence of natively occurring fluorophores.<sup>4</sup> For example, the cyanine and porphyrin dye series have found applications in photochemistry,<sup>5</sup> image-guided surgery,<sup>6</sup> and photodynamic therapy.<sup>7</sup> Although powerful, these scaffolds are hindered by poor chemical as well as photostability, relatively large molecular weights, and low quantum efficiencies.<sup>8</sup> By comparison, fluorescein and rhodamine, which are based on the xanthene ring system, have been well-documented as bright, low molecular weight fluorophore templates.<sup>9</sup> However, these dyes typically generate green to orange fluorescence, which has prompted numerous efforts to red-shift their emission wavelength.<sup>10</sup> One of the most common strategies employed in this area is to decrease the energy gap between highest occupied molecular orbital (HOMO) and lowest unoccupied molecular orbital (LUMO) by increasing the  $\pi$ -conjugation of the fluorophore. However this method typically results in a decrease in brightness ( $\epsilon \times \phi$ ) of the resulting fluorophores.<sup>11</sup> An alternative strategy for modulating the emission wavelength of xanthene-based dyes

such as rhodamine is to replace the bridging oxygen atom with other elements. Chalcogens like sulfur, selenium, and tellurium<sup>12</sup> along with group 14 elements like carbon,<sup>13</sup> silicon, germanium, and tin<sup>14</sup> have been incorporated in this manner and the resulting fluorophores all display red-shifted excitation and emission spectra compared to the parent rhodamine scaffold. However, this approach can also negatively impact the brightness of the resulting fluorophore in certain cases (Table S1 †). In addition, the exploration of new chemical handles in NIR scaffolds could enrich the tools available for fundamental biomedical research. Thus, more work is needed to identify robust and malleable NIR scaffolds for applications in chemical biology.

Inspired by the replacement of the bridging xanthene oxygen of tetramethylrhodamine (TMR) with varying elements, we envisioned a potential NIR scaffold in which the bridging xanthene oxygen of TMR was replaced by the group 15 element phosphorous. We termed these dyes the Nebraska Red (NR) series (Fig. 1). Remarkably, although phosphorous translates to “light-bringer” in Greek, fluorophores containing this element have been relatively underexplored.<sup>15-17</sup> We hypothesized that the use of a phosphinate functionality may provide an additional reactive handle on the scaffold that could be leveraged to produce changes in the spectral as well as physical properties of the dye. As an initial test of our hypothesis, we synthesized **NR<sub>666</sub>** and its ethyl ester

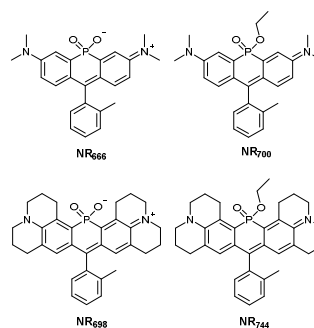


Fig. 1 Structures of Nebraska Red dye series.

<sup>a</sup> Department of Chemistry, University of Nebraska-Lincoln, Lincoln, NE 68588 (USA). E-mail: cstains2@unl.edu

<sup>b</sup> Nebraska Center for Materials and Nanoscience, University of Nebraska-Lincoln, Lincoln, NE 68588 (USA)

† Electronic Supplementary Information (ESI) available: Synthesis and characterization of new compounds, experimental details, and supplementary figures. See DOI: 10.1039/x0xx00000x

## COMMUNICATION

Journal Name

counterpart **NR**<sub>700</sub> (Scheme 1). Investigation of the photophysical properties of these two dyes showed that both dyes absorbed and emitted in the NIR region in aqueous solutions (Fig. 2a-c). Moreover, we observed a red-shift in both the excitation and emission spectra of **NR**<sub>700</sub> compared to **NR**<sub>666</sub>. The molar extinction coefficients and quantum yields of both dyes were determined and, in particular, **NR**<sub>666</sub> was found to be 1.3-fold brighter than the parent TMR scaffold (Table S1 †).<sup>11</sup> In addition, **NR**<sub>666</sub> was stable to continuous irradiation for 1 hr (Fig. 2d). Over the same time period we observed a decrease in **NR**<sub>700</sub> fluorescence, similar to the commonly used Cy 5.5 dye (Fig. 2d). Further investigation indicated that the decrease in fluorescence of **NR**<sub>700</sub> was due to autohydrolysis of the phosphinate ester, yielding **NR**<sub>666</sub> (Fig. S1a, ESI †). Monitoring conversion of **NR**<sub>700</sub> to **NR**<sub>666</sub> yielded a first-order rate of 0.026 min<sup>-1</sup> for hydrolysis (Fig. S1b, ESI †). These experiments demonstrate that the ether substituents on the phosphinate of NR dyes can be used to modulate fluorescence and could potentially be exploited as additional sites for modification of the physical properties of these dyes. Computational calculations showed that introduction of the phosphinate functionality resulted in stabilization of dye LUMO energies relative to the parent TMR scaffold, providing a mechanism for the red-shift observed in these fluorophores (Fig. S2 †).

Encouraged by these initial results, we set out to identify dyes with excitation and emissions above 700 nm by replacing the dimethylaniline functionality of our initial NR dyes with a julolidine substituent. Accordingly, we synthesized **NR**<sub>698</sub> and its phosphinate ethyl ester counterpart, **NR**<sub>744</sub> (detailed synthetic procedures in the ESI †). Satisfyingly, both these derivatives displayed excitation and emission peaks at or above 700 nm and maintained the photostability of the parent xanthene scaffold (Fig. 2). Interestingly, we did not observe spontaneous hydrolysis of **NR**<sub>744</sub> during the timeframe of our experiment. The resistance of **NR**<sub>744</sub> to hydrolysis may be a result of increased steric bulk and is currently under further investigation. Nonetheless, these results demonstrate that the phosphinate functionality can be utilized as a transposable element in fluorophore design.

To investigate the potential sensitivity of phosphinate-containing dyes to changes in pH, we determined the fluorescence of **NR**<sub>666</sub> and **NR**<sub>698</sub> at varying pHs (Fig. S3, ESI †). Low pHs induced a red-shift in the excitation and emission wavelength of both dyes as well as a decrease in fluorescence

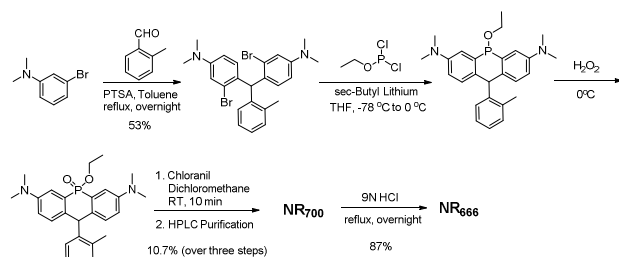
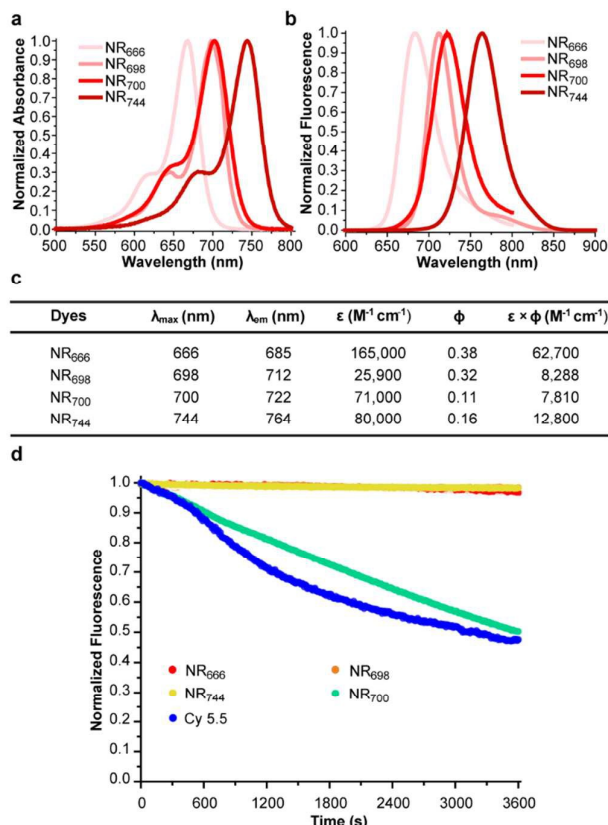
Scheme 1 Synthesis of **NR**<sub>666</sub> and **NR**<sub>700</sub>.

Fig. 2 Photophysical properties of the NR dye series. All experiments were performed in PBS (10 mM, pH = 7.4 with 1% DMSO). (a) Absorption spectra. (b) Emission spectra. (c) Summary of optical parameters. (d) Photostability comparison with Cy 5.5.

intensity, yielding mid-points of 0.5 and 1.8 pH units for **NR**<sub>666</sub> and **NR**<sub>698</sub>, respectively. Based on these measurements, both dyes can be used under physiological conditions with essentially no inference due to changes in pH. Taken together, the NR template displays remarkable photostability compared to commonly employed NIR fluorophores,<sup>18</sup> providing a robust scaffold for the design of NIR dyes.

Building upon the observation that **NR**<sub>700</sub> underwent spontaneous hydrolysis to yield **NR**<sub>666</sub>, we asked whether phosphinate ester substituents could be used to tune the physical properties of NR dyes, such as cell permeability. Accordingly, we incubated HeLa cells with either **NR**<sub>666</sub> or **NR**<sub>700</sub>. Gratifyingly, cell uptake was only observed for the **NR**<sub>700</sub> derivative, indicating that phosphinate ester substituents can be used to modulate the cell permeability of NR dyes (Fig. 3). Our laboratory is currently pursuing this approach to afford a suite of cell permeable and impermeable reagents for labelling studies.

Lastly, we sought to demonstrate a proof-of-principle for generation of a self-reporting small molecule delivery reagent using **NR**<sub>666</sub> as a template. Given our laboratory's interest in detecting biologically relevant signalling molecules,<sup>19-20</sup> we chose to demonstrate the utility of the NR scaffold by developing a reagent that would deliver a small molecule in response to a biologically relevant stimulus. Reactive oxygen species (ROS) and reactive nitrogen species (RNS) represent a

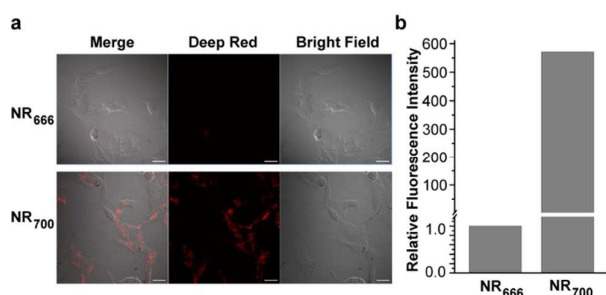
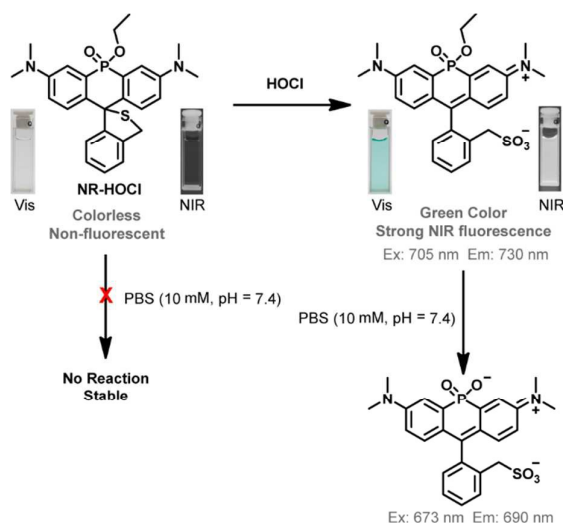


Fig. 3 Cell permeability comparison between **NR<sub>666</sub>** and **NR<sub>700</sub>**. (a) Living HeLa cells were incubated with 5  $\mu\text{M}$  dye for 15 min at 37  $^{\circ}\text{C}$  followed by washing with PBS (3x). Scale bar: 25  $\mu\text{m}$ . (b) The average fluorescence intensity of cells from panel a.

group of small molecules that are associated with numerous human diseases.<sup>21</sup> HOCl, a member of the ROS family, causes inflammation at the site of tissue injury due to its strong oxidative properties.<sup>22</sup> Building upon previously reported fluorescent sensors for HOCl,<sup>23-26</sup> we sought to construct a self-reporting small molecule delivery reagent triggered by HOCl. Combining the selective reaction of spirocyclic thioethers with HOCl<sup>27-33</sup> and the NIR properties of the NR scaffold, we envisioned a reagent that would remain intact and non-fluorescent until reaction with HOCl. Importantly, we anticipated that this reagent, termed **NR-HOCl** (detailed synthetic procedures in the ESI<sup>†</sup>), would spontaneously hydrolyze upon reaction with HOCl to yield ethanol and **NR<sub>666</sub>** (Scheme 2). Indeed, **NR-HOCl** was found to be non-fluorescent until exposure to HOCl, which yielded a product with excitation and emission maxima at 705 and 730 nm, respectively (Scheme 2 and Fig. S4, ESI<sup>†</sup>). **NR-HOCl** was highly selective for HOCl compared to excess off-target ROS and RNS (Fig. S5, ESI<sup>†</sup>). Titration experiments revealed that the limit of detection of **NR-HOCl** for HOCl is 3 nM (Fig. S6, ESI<sup>†</sup>), well below physiologically relevant concentrations of HOCl (5 - 50  $\mu\text{M}$ ).<sup>34</sup> **NR-HOCl** also was capable of detecting HOCl across a wide range of pHs (3 - 9) with a maximum increase in fluorescence at pH 7 (Fig. S7, ESI<sup>†</sup>). As expected, incubation of **NR-HOCl** after treatment with HOCl resulted in hydrolysis of its phosphinate ester, providing a final product with excitation and emission maxima at 673 and 690 nm, respectively (Fig. S4, ESI<sup>†</sup>). The phosphinate ester of **NR-HOCl** remained intact after 24 hrs in the absence of HOCl (Scheme 2 and Fig. S8, ESI<sup>†</sup>).

Confident in the ability of **NR-HOCl** to selectively react with HOCl and subsequently undergo phosphinate ester hydrolysis, we next asked whether this reagent could function in the context of living cells. As an initial trial, HeLa cells were incubated with **NR-HOCl** and HOCl was subsequently added. A distinct “off-on” signal was observed in presence of HOCl (Fig. S9, ESI<sup>†</sup>), demonstrating that **NR-HOCl** could self-report on small molecule delivery in living cells in response to an exogenous HOCl input. Importantly, no cellular toxicity was observed from **NR-HOCl** alone at the concentrations used in these experiments (Fig. S10, ESI<sup>†</sup>). Bolstered by these results



Scheme 2 Cleavage of **NR-HOCl** phosphinate ester upon reaction with HOCl.

we sought to determine whether the production of endogenous HOCl by macrophages (RAW 264.7) stimulated with lipopolysaccharide (LPS) and phorbol 12-myristate 13-acetate (PMA) would be capable of triggering small molecule release. These experiments yielded a clear increase in cellular **NR-HOCl** fluorescence that was proportional to the amount of stimuli applied, validating the potential to self-report on small molecule release using endogenous HOCl as a stimulus (Fig. 4). These results indicate the intriguing possibility of utilizing the NR scaffold as a potential template for reaction-induced release of small molecules capable of eliciting a biological response. We are currently investigating this application in our laboratory.

## Conclusions

In summary, we have developed a novel NIR fluorophore scaffold that shows remarkable brightness and photostability under physiological conditions. The generality of our design

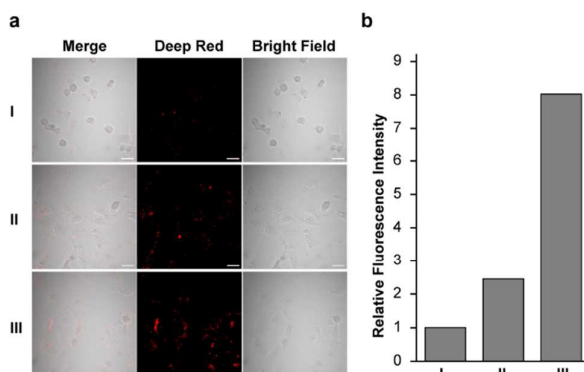


Fig. 4 (a) Confocal fluorescence microscopy imaging of living RAW 264.7 cells incubated with 10  $\mu\text{M}$  **NR-HOCl** and (I) without LPS or PMA, (II) with LPS (1  $\mu\text{g}/\text{mL}$ ) and PMA (0.1  $\mu\text{g}/\text{mL}$ ), or (III) with LPS (1  $\mu\text{g}/\text{mL}$ ) and PMA (1  $\mu\text{g}/\text{mL}$ ) induction. Scale bar: 25  $\mu\text{m}$ . (b) The average fluorescence intensity of cells from panel a.

approach was demonstrated by developing four new NIR dyes. Given the prevalence of bridging oxygens in fluorophore structures, we anticipate the ability to generate a diverse color pallet via introduction of phosphinate functionalities into existing fluorophores. We further demonstrated the chemical utility of the phosphinate functionality by controlling physical properties such as cell permeability as well as generating self-reporting small molecule delivery reagents. We anticipate that the Nebraska Red template will provide a robust scaffold for the further development of chemical biology tools.

### Acknowledgements

We acknowledge the Morrison Microscopy Core Research Facility and Christian Elowsky for assistance with confocal fluorescence microscopy as well as Prof. Edward Harris for use of cell culture equipment. We also thank the Research Instrumentation/NMR facility and the Nebraska Center for Mass Spectrometry for assistance with characterization of new compounds. Calculations were performed with resources at the University of Nebraska-Lincoln Holland Computing Center. This work was funded by the NIH (R35GM119751), the University of Nebraska-Lincoln, and the Center for Nanohybrid Functional Materials (NSF EPS-1004094).

### Notes and references

- J. Chan, S. C. Dodani and C. J. Chang, *Nat. Chem.*, 2012, **4**, 973-984.
- J. B. Grimm, L. M. Heckman and L. D. Lavis, in *Progress in Molecular Biology and Translational Science*, ed. C. M. May, Academic Press, 2013, vol. Volume 113, pp. 1-34.
- H. Kobayashi, M. R. Longmire, M. Ogawa and P. L. Choyke, *Chem. Soc. Rev.*, 2011, **40**, 4626-4648.
- F. L. Tansi, R. Ruger, M. Rabenhold, F. Steiniger, A. Fahr, W. A. Kaiser and I. Hilger, *Small*, 2013, **9**, 3659-3669.
- A. P. Gorka, R. R. Nani, J. J. Zhu, S. Mackem and M. J. Schnermann, *J. Am. Chem. Soc.*, 2014, **136**, 14153-14159.
- J. T. Alander, I. Kaartinen, A. Laakso, T. Patila, T. Spillmann, V. V. Tuchin, M. Venermo and P. Valisuo, *Int. J. Biomed. Imaging*, 2012, **2012**, 940585.
- J. Schmitt, V. Heitz, A. Sour, F. Bolze, H. Ftouni, J. F. Nicoud, L. Flamigni and B. Ventura, *Angew. Chem. Int. Edit.*, 2015, **54**, 169-173.
- J. O. Escobedo, O. Rusin, S. Lim and R. M. Strongin, *Curr. Opin. Chem. Biol.*, 2010, **14**, 64-70.
- A. Zumbuehl, D. Jeannerat, S. E. Martin, M. Sohrmann, P. Stano, T. Vigassy, D. D. Clark, S. L. Hussey, M. Peter, B. R. Peterson, E. Pretsch, P. Walde and E. M. Carreira, *Angew. Chem. Int. Edit.*, 2004, **43**, 5428-5428.
- M. Sibrían-Vázquez, J. O. Escobedo, M. Lowry, F. R. Fronczek and R. M. Strongin, *J. Am. Chem. Soc.*, 2012, **134**, 10502-10508.
- L. D. Lavis and R. T. Raines, *ACS Chem. Biol.*, 2008, **3**, 142-155.
- M. W. Kryman, G. A. Schamerhorn, J. E. Hill, B. D. Calitree, K. S. Davies, M. K. Linder, T. Y. Ohulchanskyy and M. R. Detty, *Organometallics*, 2014, **33**, 2628-2640.
- J. B. Grimm, T. D. Gruber, G. Ortiz, T. A. Brown and L. D. Lavis, *Bioconjugate Chem.*, 2016, **27**, 474-480.
- Y. Koide, Y. Urano, K. Hanaoka, T. Terai and T. Nagano, *ACS Chem. Biol.*, 2011, **6**, 600-608.
- E. Yamaguchi, C. G. Wang, A. Fukazawa, M. Taki, Y. Sato, T. Sasaki, M. Ueda, N. Sasaki, T. Higashiyama and S. Yamaguchi, *Angew. Chem. Int. Edit.*, 2015, **54**, 4539-4543.
- A. Fukazawa, S. Suda, M. Taki, E. Yamaguchi, M. Grzybowski, Y. Sato, T. Higashiyama and S. Yamaguchi, *Chem. Commun.*, 2016, **52**, 1120-1123.
- X. Chai, X. Cui, B. Wang, F. Yang, Y. Cai, Q. Wu and T. Wang, *Chem.-Eur. J.*, 2015, **21**, 16754-16758.
- M. Sauer, J. Hofkens and J. Enderlein, in *Handbook of Fluorescence Spectroscopy and Imaging*, Wiley-VCH Verlag GmbH & Co. KGaA, 2011, pp. 1-30.
- J. R. Beck, A. Lawrence, A. S. Tung, E. N. Harris and C. I. Stains, *ACS Chem. Biol.*, 2016, **11**, 284-290.
- X. Zhou, R. Lai, H. Li and C. I. Stains, *Anal. Chem.*, 2015, **87**, 4081-4086.
- P. T. Schumacker, *Cancer Cell*, 2015, **27**, 156-157.
- F. Dallegri and L. Ottonello, *Inflamm. Res.*, 1997, **46**, 382-391.
- Y. Zhou, J. Y. Li, K. H. Chu, K. Liu, C. Yao and J. Y. Li, *Chem. Commun.*, 2012, **48**, 4677-4679.
- L. Yuan, W. Y. Lin, Y. N. Xie, B. Chen and J. Z. Song, *Chem.-Eur. J.*, 2012, **18**, 2700-2706.
- Y. R. Zhang, N. Meng, J. Y. Miao and B. X. Zhao, *Chem.-Eur. J.*, 2015, **21**, 19058-19063.
- Q. Xu, K. A. Lee, S. Lee, K. M. Lee, W. J. Lee and J. Yoon, *J. Am. Chem. Soc.*, 2013, **135**, 9944-9949.
- Q. A. Best, N. Sattenapally, D. J. Dyer, C. N. Scott and M. E. McCarroll, *J. Am. Chem. Soc.*, 2013, **135**, 13365-13370.
- S. Kenmoku, Y. Urano, H. Kojima and T. Nagano, *J. Am. Chem. Soc.*, 2007, **129**, 7313-7318.
- Y. Koide, Y. Urano, K. Hanaoka, T. Terai and T. Nagano, *J. Am. Chem. Soc.*, 2011, **133**, 5680-5682.
- X. Zhan, J. Yan, J. Su, Y. Wang, J. He, S. Wang, H. Zheng and J. Xu, *Sens. Actuators B Chem.*, 2010, **150**, 774-780.
- J. Zhou, L. Li, W. Shi, X. Gao, X. Li and H. Ma, *Chem. Sci.*, 2015, **6**, 4884-4888.
- X. Chen, K. A. Lee, E. M. Ha, K. M. Lee, Y. Y. Seo, H. K. Choi, H. N. Kim, M. J. Kim, C. S. Cho, S. Y. Lee, W. J. Lee and J. Yoon, *Chem. Commun.*, 2011, **47**, 4373-4375.
- X. Li, X. Gao, W. Shi and H. Ma, *Chem. Rev.*, 2014, **114**, 590-659.
- J. M. Davies, D. A. Horwitz and K. J. Davies, *Free Radic. Biol. Med.*, 1993, **15**, 637-643.